Intermittent reduction in ocean heat transport into the Getz Ice Shelf cavity during strong wind events

Nadine Steiger[1,2] (nadine.steiger@uib.no), Elin Darelius[1,2], Anna Wåhlin[3] and Karen Assmann[4]

Observations in front of the western Getz Ice Shelf show eight intermittent events of Winter Water deepening during the winter of 2016. The events are driven by non-local coastal Ekman downwelling and they reduce the ocean heat transport into the cavity by 25% during that winter.

[1]Geophysical Institute, University of Bergen, Norway
[2]Bjerknes Centre for Climate Research, Bergen, Norway
[3]Department of Marine Sciences, University of Gothenburg, Sweden
[4] Institute of Marine Research, Tromsø, Norway

Foto credit: NASA

DATA – Two years of mooring records at the front of the Getz Ice Shelf

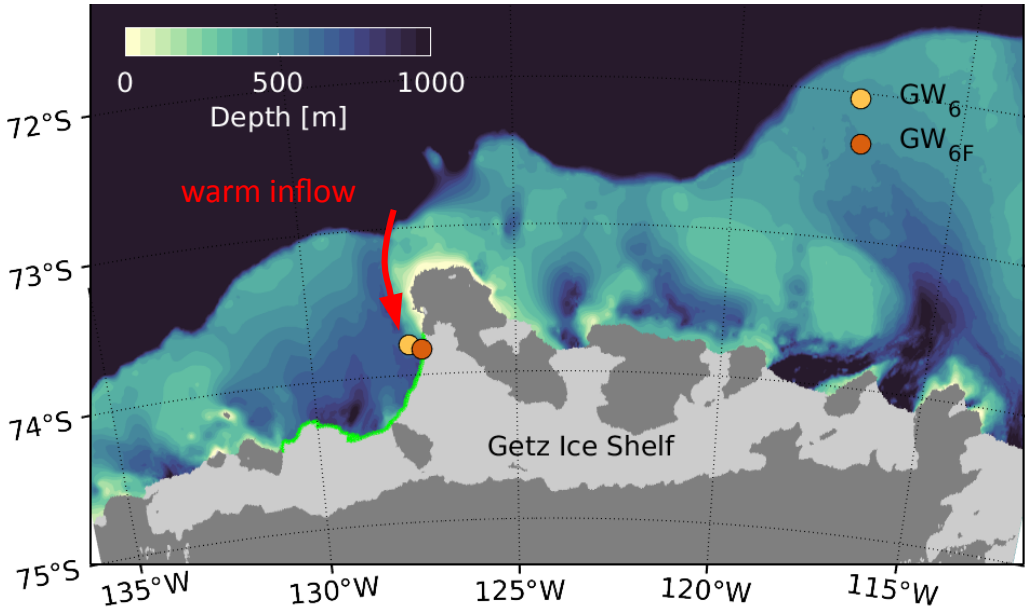

Figure 1: *IBCSO-Bathymetry (Arndt et al. 2013) of the continental shelf in the Getz Ice Shelf region and the location of the two moorings.*

Two moorings (GW_6 & GW_{6F}) measured hydrography and currents in front of the Getz Ice Shelf from January 2016 to January 2018.

There is a **persistent inflow of warm CDW** during these two years (Assmann et al. 2019), transported towards the ice shelf by a current that has a barotropic and a baroclinic component. The barotropic component is blocked at the ice front (Wåhlin et al. 2020).

The inflow is in addition **disrupted by events of strongly deepened Winter Water**. In this study, investigate the drivers of these events and the implications for the heat transport into the ice shelf cavity.

OBSERVATIONS – Events with Winter Water deepening

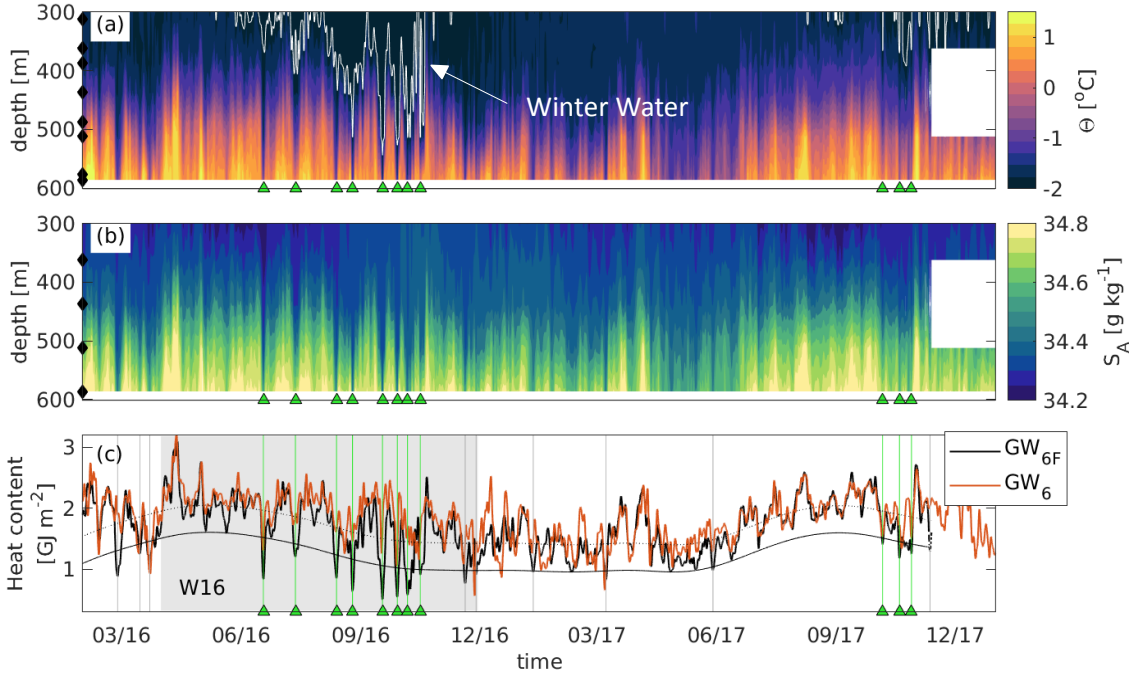

Figure 2: *Timeseries of (a) conservative temperature and (b) absolute salinity at the mooring GW_{6F} and the heat content between 300-600m depth at GW_6 and GW_{6F}. The events of deepened Winter Water are marked as ▲.*

The temperature at the bottom is relatively high, but in the winter of 2016 (W16) **the Winter Water reaches below 350 m depth with intermittent deepening far towards the bottom** (Fig. 2a).

Salinity decreases at depth during the events (Fig. 2b).

In W16 there are eight events* ▲ that are visible at both moorings as sharp drops in the heat content (Fig. 2c) .

What drives the events of deepened Winter Water during W16?

*We identify events as local minima in heat content at GW_{6F} below one standard deviation from the 90-day lowpass filtered heat content during periods when the WW is deeper than 350 m.

DRIVERS – The events coincide with strong easterly winds and coastal polynya opening

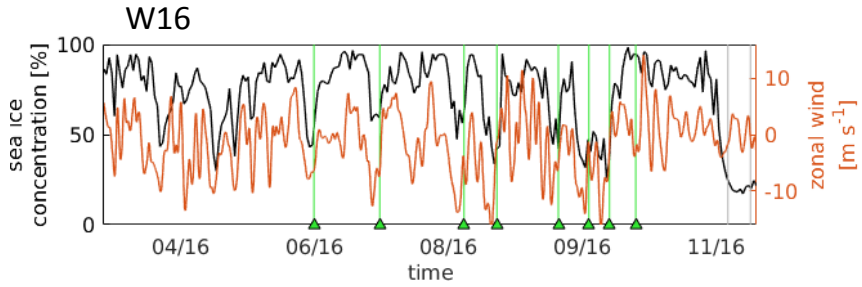

Figure 3: *Timeseries of local zonal winds from ERA5 (Hersbach et al. 2018) and high resolution sea ice concentration from University of Bremen (Spreen et al. 2008) during W16.*

The winds in the Getz Ice Shelf region are generally easterly.

During the events, **strong easterly winds of about 12 m s^{-1} open a coastal polynya** at the ice front and north of Siple Island.

How do the polynya and the winds influence the hydrography at the mooring site?

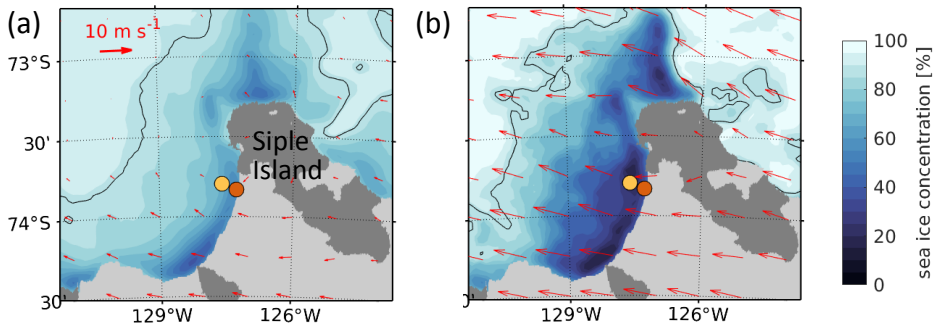

Figure 4: *Winds and sea ice concentration (a) averaged over W16 and (b) averaged over 3 days before all events. The contours of the 90% sea ice concentration is marked.*

DRIVERS – Influence of the polynyas on the hydrography

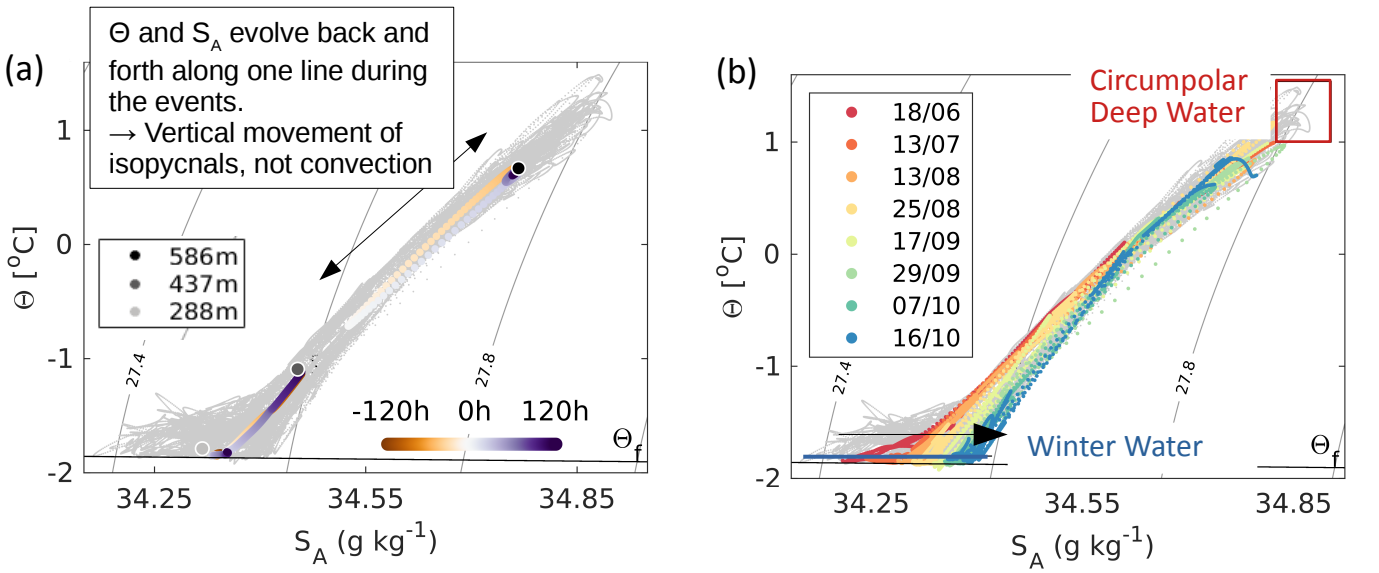

Figure 5: *Temperature-salinity plot of the two year measurements at GW_{6F} (grey dots) and (a) an ensemble of the events (120h before and after) at three depths (color) and (b) each of the events during W16 (color).*

Each of the short events causes a **vertical movement of isopycnals** (Fig. 5a).

The frequent polynya opening throughout the winter of 2016 densifies the Winter Water (WW) throught the winter (Fig. 5b).

DRIVERS – Surface heat transport

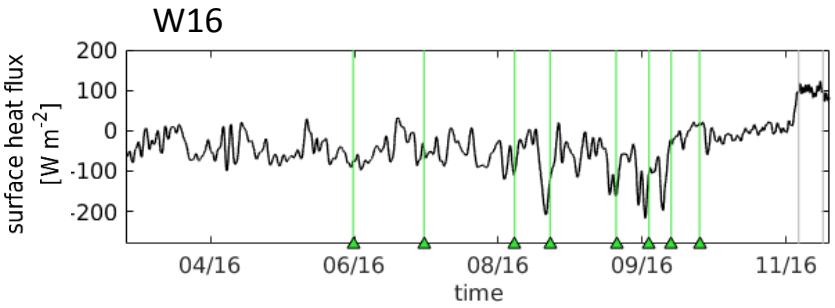

Figure 6: *Time series of the surface heat flux from ERA5 at the mooring site during W16.*

Cumulative surface heat flux at the mooring site: 0.02 GJ m^{-2}
Change in heat content at the mooring site during an event: ~ 1 GJ/m^{-2}

The surface heat fluxes (ERA5) show drops during some of the events, but the **cumulated surface heat flux during each of the events is two orders of magnitude smaller** than the drop in ocean heat content.

DRIVERS – The influence of strong easterly winds

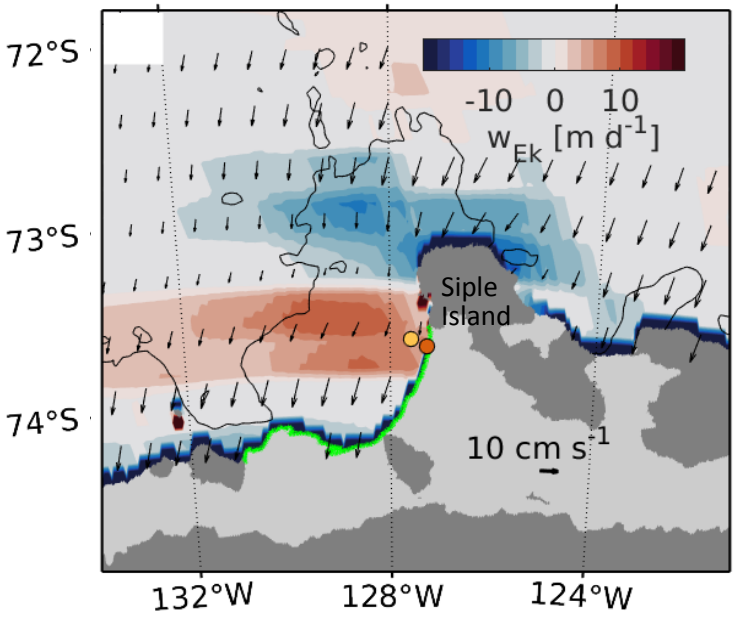

Figure 7: *Ekman transport (arrows) and vertical Ekman velocities (w_{Ek}) calculated from the 10m winds.*

The easterly winds induce upwelling at the mooring site (red colors in Fig. 7), not downwelling. Strong downwelling (blue colors in Fig. 7) occurs along other parts of the coast and north of Siple Island.

We suggest that the **on-shore Ekman transport north of Siple Island drives the deepening of the Winter Water** and the signal propagates along the coast towards the mooring site as a **coastal trapped wave**.

Observed wave speed: $c = \frac{100\,km}{50-70\,h} = 0.4-0.6\,m\,s^{-1}$

Theoretical speed:

Internal Kelvin wave: $c = \sqrt{g' \frac{H_1 H_2}{H_1 + H_2}} \approx 0.4-0.6\,m\,s^{-1}$

Topographic Rossby wave: $c = g' \frac{\alpha}{f} \approx 0.2-0.4\,m\,s^{-1}$

IMPLICATIONS - Heat transport into the ice shelf cavity

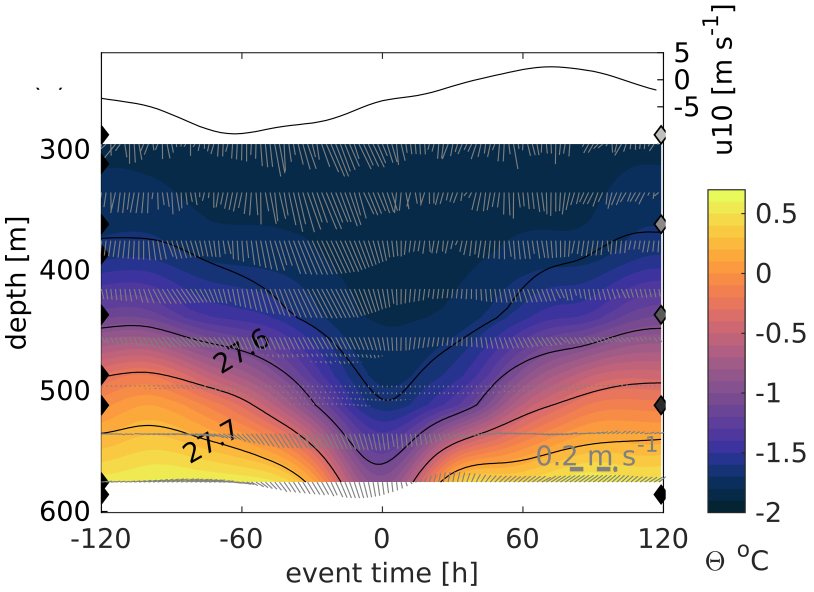

Figure 8: *Ensemble of the events in W16. Conservative temperature (color), density (contours) and velocity (feathers) at GW_{6F} (pointing up is north) together with the 10m zonal wind (u10).*

The isotherms and isopycnals deepen about 60h after the peak in easterly winds. (Fig. 8)

While the isotherms deepen, the currents at all depths changes direction.

At depth (>400m), warm water typically enters the cavity, but **during the events the water is colder and the current aligns with the ice front**. (Fig. 9)

The heat transport into the Getz Ice Shelf cavity is reduced by 25% due to the events.

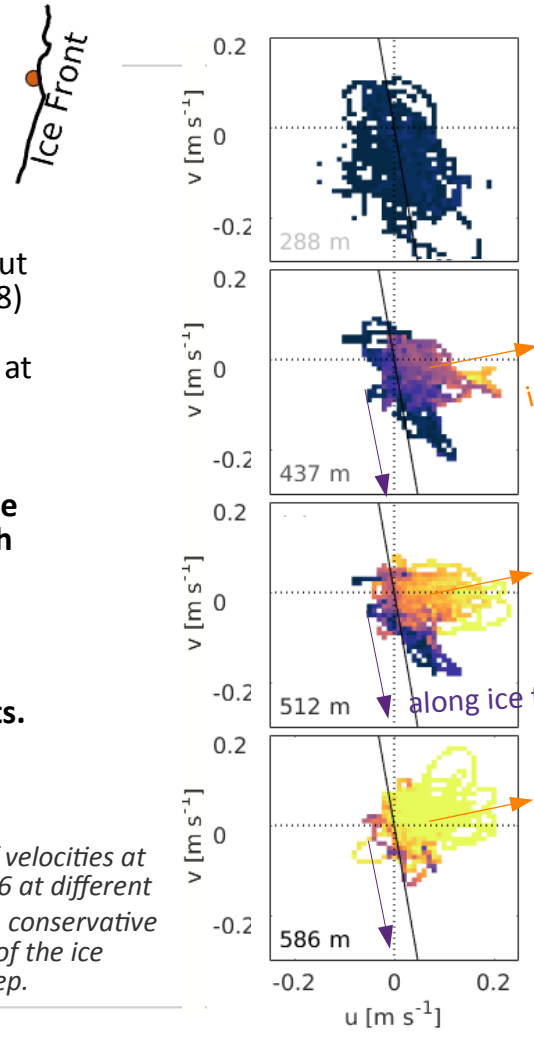

Figure 9: *Scatter plot of velocities at GW_{6F} during winter 2016 at different depths color coded with conservative temperature. The base of the ice shelf is about 300 m deep.*

INTERANNUAL VARIABILITY

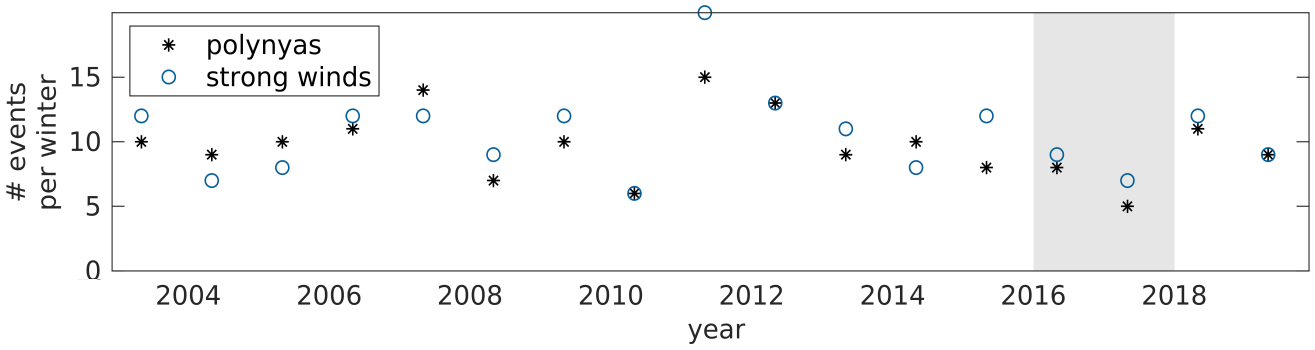

Figure 10: *Number of polynyas (drops of 7-day lowpass filtered sea ice concentration below 70%) and number of strong easterly winds (peaks in 7-day lowpass filtered easterly winds larger than the time-mean of easterly winds) during each winter from 2003 to 2019.*

In winter 2017 the mooring time series shows less events of deepened Winter Water and there were less winter polynas and fewer strong easterly winds compared to winter 2016 (Fig. 2).

Compared to other years, the 2016-conditions are more common and there is potential for more events in other years.

In addition to these atmospheric conditions, the preconditioning of the water column (i.e. stratification) determines the effect of strong winds on the deepening of the Winter Water.

SUMMARY

average winter conditions

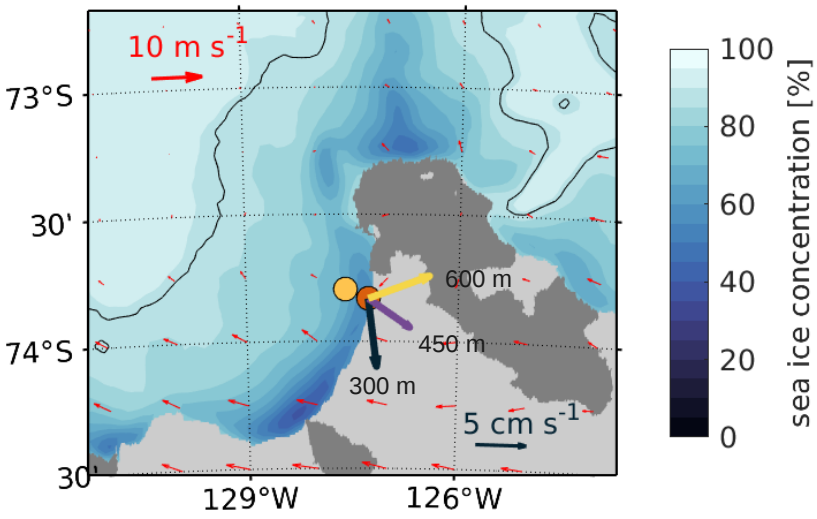

The baroclinic component that enhances the current at depth, where the warm water is contained, enters the ice shelf cavity (Wåhlin et al. 2020).

events of deepened Winter Water

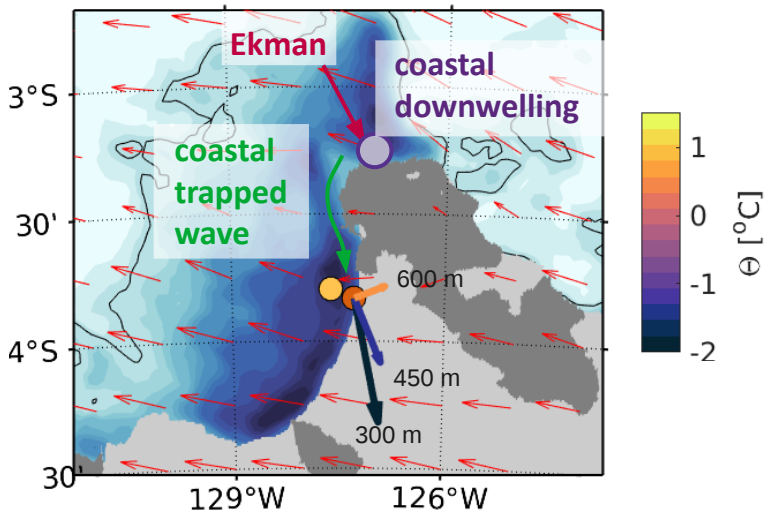

Strong easterly winds cause on-shore Ekman transport and coastal downwelling north of Siple Island.
The signal of deepend Winter Water propagates as a coastal trapped wave towards the mooring site.
The bottom temperature drops by 1-2°C – The Winter Water deepens and the currents aligns with the ice shelf front as the baroclinic component is reduced.

REFERENCES

Arndt, J. E., Schenke, H. W., Jakobsson, M., Nitsche, F. O., Buys, G., Goleby, B., . . . Wigley, R. (2013). The international bathymetric chart of the Southern Ocean (IBCSO) version 1.0-A new bathymetric compilation covering circum-Antarctic waters. Geophysical Research Letters, 40 (12), 3111–3117. doi: 10.1002/grl.50413

Assmann, K. M., Darelius, E., Wåhlin, A., Kim, T. W., & Lee, S. H. (2019). Warm Circumpolar Deep Water at the Western Getz Ice Shelf Front , Antarctica. Geophysical Research Letters, 46 (2), 870–878. doi: 10.1029/2018GL081354

Hersbach, H., Bell, B., Berrisford, P., Biavati, G., Horányi, A., Muñoz Sabater, J., . . . Thépaut, J.-N. (2018). ERA5 hourly data on single levels from 1979 to present. Copernicus Climate Change Service (C3S) Climate Data Store (CDS) (Accessed on 11-Sep-2020). doi: 10.24381/cds.adbb2d47

Spreen, G., Kaleschke, L., & Heygster, G. (2008). Sea ice remote sensing using AMSR-E 89-GHz channels. Journal of Geophysical Research: Oceans, 113 (2), 1–14. doi: 10.1029/2005JC003384

Wåhlin, A. K., Steiger, N., Darelius, E., Assmann, K. M., Glessmer, M. S., Ha, H. K., . . . Viboud, S. (2020). Ice front blocking of ocean heat transport to an Antarctic ice shelf. Nature, 578 , 568—-571. doi: 10.1038/s41586-020-2014-5